UDC 549:553.2

CAVITATION MODEL OF MINERAL MICROSPHERULA FORMATION IN HYDROTHERMAL ORES

Margarita I. Novgorodova
Fersman Mineralogical Museum of the Russian Academy of Science, Moscow, min@fmm.ru
Stepan N. Andreev, Alexander A. Samokhin
Intitute of General Physics of the Russian Academy of Science, Moscow, asam@ran.gpi.ru

The cavitation model was considered to explain mineral microspherula formation conditions in ores of hydrothermal genesis. Microspherulas are treated as hardened and crystallized drops of melt. Thermodynamic calculations of thermal energy emitted during microseconds at gas bubble contraction in boiling up hydrothermal solution show that fusion of such refractory substances as quartz and gold is possible.
2 tables, 6 figures and 12 references

Mineral microspherulas of micrometer size (from 10 to 100 μm in diameter) of different mineral composition were known from a long time (Vernadsky, 1955), but they have caused a special interest after were discovered directly in ores at a great depth (Gamyanin *et al.*, 1999; Novgorodova *et al.*, 2003). Earlier various reasons were used to explain their formation. So-called magnetic balls consisting of native iron with admixture of Ni, frequently completely or in part replaced with wьstite or magnetite, were considered of cosmogenic origin; that found in mechanically crashed ores were considered as technogenous artifacts (Dilabio *et al.*, 1988). Rounded concretion forms of mineral aggregates are well-known for sedimentary ores and mineral deposits of karst caves (cave pearls). None of these explanations can be used to explain conditions in which microspherulas of alumosilicate glasses and refractory metals, as well as sulfides settling down in voids and cracks of α-quartz veins, were formed in mineralized zones of terrigenous and volcanosedimentary rocks metamorphosed to greenschist facies (gold deposits of Yakutia, West Uzbekistan, Alaska). Boundary parameters of greenschist metamorphism (T up to ~500°C, P up to ~2—8 kbar) do not suppose formation of conditions for partial melting of sulfide ores, as it was assumed by R. Frost (Frost *et al*, 2002) for deposits in rocks of amphibolitic and granulitic facies of metamorphism.

Actual data on physicochemical parameters of ore-forming solutions give thermobarometric studies of gas-liquid inclusions in minerals, in particular, in quartz. At the well studied Nezhdaninskoye deposits (Yakutia) it was established that ores were formed at T 175—360°C and P 1.2—1.7 kbar at participation from medium salted solutions with $H_2O>CO_2>CH_4 = N_2>H_2S$, separated into two phases: liquid water-carbon dioxide with N_2, CH_4, dissolved chlorides, and gaseous with prevailing CO_2 and CH_4 (Bortnikov *et al.*, 1998). Quartz grains do not show signs of fusion of quartz.

To explain formation of alumosilicate glass and refractory metal microspherulas with fusion points essentially exceeding temperature of hydrothermal solution at formation of gold-ore mesothermal deposits (Nezhdaninskoyee, Kellyam in Yakutia, Kokpatas in West Uzbekistan, Democrat on Alaska) a hypothesis on cavitation nature of the phenomenon was put forward (Novgorodova *et al.*, 2003_1).

It was assumed that mineral microspherulas have been formed due to fast cooling and crystallization of melt drops arising in local zones of slightly open cracks and voids in the mineralization zone due to the phenomena of cavitation boiling up and heterogenization of hydrothermal solutions. The transition from a regime of slow infiltration of hydrothermal solutions through capillaries and pores in hosting rock to instant filling of cracks slightly opened at tectonic movements results in local pressure decrease, expansion of evolved gas bubbles and their collapse at returning to former conditions at full filling of slightly opened space. After the collapse, fine bubbles disappear, large are broken into a set of fine ones. Time of one bubble cycle is estimated at microseconds, however, heat and energy necessary for fusion of either solid particle in the impact zone of collapsing bubble are sufficient for fusion of such refractory matter, as quartz or gold. This is shown by the calculations below.

Fused state of microspherulas prior to their hardening and crystallization was established basing on the following facts and reasons (Novgorodova *et al.*, $2003_{1,2}$).

Alumosilicate glasses of microspherulas (Fig. 1) are transparent, non-crystalline characterized by wide variety and discreteness in contents of rock-forming elements depleted in sili-

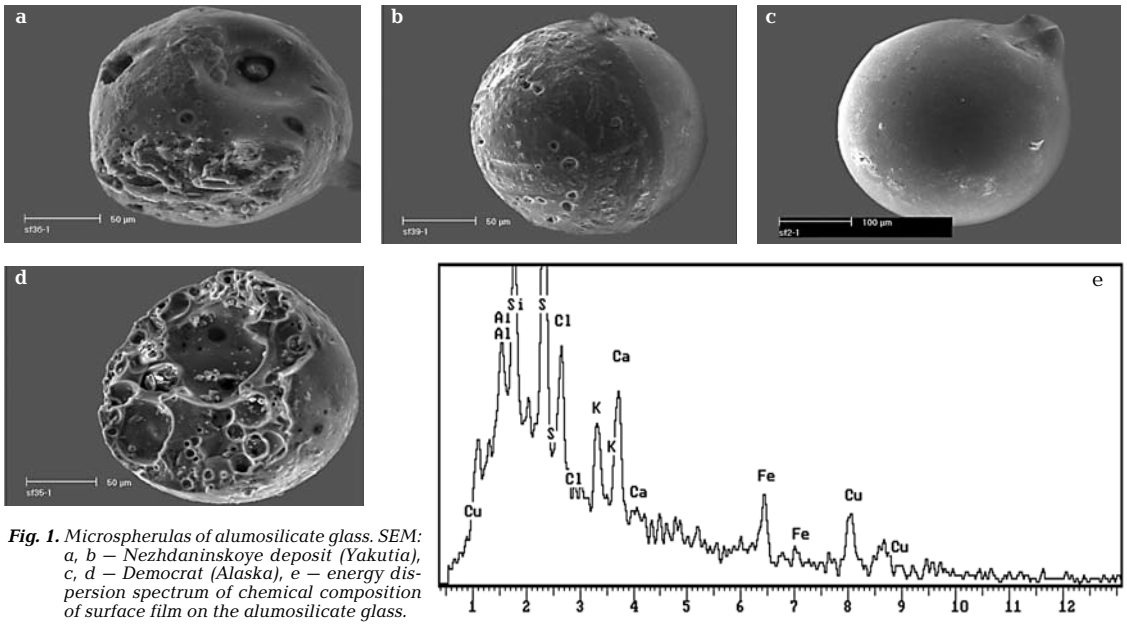

Fig. 1. *Microspherulas of alumosilicate glass. SEM: a, b — Nezhdaninskoye deposit (Yakutia), c, d — Democrat (Alaska), e — energy dispersion spectrum of chemical composition of surface film on the alumosilicate glass.*

ca and alkalis as against the gold-hosting rocks and enriched with femic components (Fig. 2). The most part of analyses does not correspond to known chemical composition of any magmatic rock. The internal irregularity of microspherula chemical composition with inclusions of glass in glass was revealed; inclusions have low SiO_2 content and are represented by discrete compositions with high contents of Al_2O_3, MgO, CaO, FeO.

Microspherulas of monomineral composition were revealed among alumosilicate glasses. At the Nezhdaninskoye deposit, they are represented by glasses of almost pure SiO_2 (98.69—99.02 %) and pyroxene of enstatite-bronzite type with stoichiometric formula $(Mg_{1.4}Fe_{0.6})_2(Si_{1.9}Al_{0.1})_2O_6$. Pyroxene is absent in terrigenous rocks containing gold-antimony ore in this deposit. All investigated glasses of the Democrat deposit have a similar formula of enstatite-bronzite.

The size of alumosilicate glass microspherulas is from 10 to 100 μm (usually ~50 μm). Quartz glass microspherulas are the finest. All microspherulas are saturated with numerous gas vacuoles. Films and ingrowths of Ca, Cu, Zn, and Fe salts with ligands containing S, Cl, P, C were discovered on their surface by scanning electronic microscopy (SEM) using energy dispersion spectrometer Zink-860 (Fig. 1).

Microspherulas of ore minerals, which compositions are described by the system Pb-Sb-Au(Ag)-S(As), are monomineral (native gold, galena, antimonite, boulangerite, pyrrhotite) and polymineral microspherulas of zonal structure with «gold» core and galena-boulangerite rims. Films of alumosilicate glasses and salts of Cu and Zn with ligands of Cl and S were discovered on their surface. Inside microspherulas, there are gas cavities and relics of quartz and arsenopyrite fragments.

Sliced and dendrite-like internal structure of monomineral microspherulas was established; contraction cracks, arising at reduction of volume at hardening and crystallization of melt gold drops (Fig. 3), are characteristic of microspherulas of native gold.

Zonal microspherulas show signs of liquation with separation of sulfide (Pb-Sb(As)-S) phase in marginal zones with eutectoid aggregates of galena and boulangerite and metal phase (Au(Ag)-Pb-Sb) part in the central zone (Fig. 4). The «gold» core is characterized by signs of stratification with sliced structure of phases differing in Pb contents and eutectoid aggregates of Au-Sb and Au-Pb-Sb phases (Table 1). The affinity of composition of natural Au-Pb-Sb phases to synthesized glasses of a new class of high-temperature superconductors was established for the first time (Novgorodova *et al.*, 2003_2).

Using systems of invariant points in fluxion diagrams (Table 2), the interval of microspherula formation temperatures was evaluated between > 850°C (fusion of gold, galena, antimony, alumosilicates and quartz at pres-

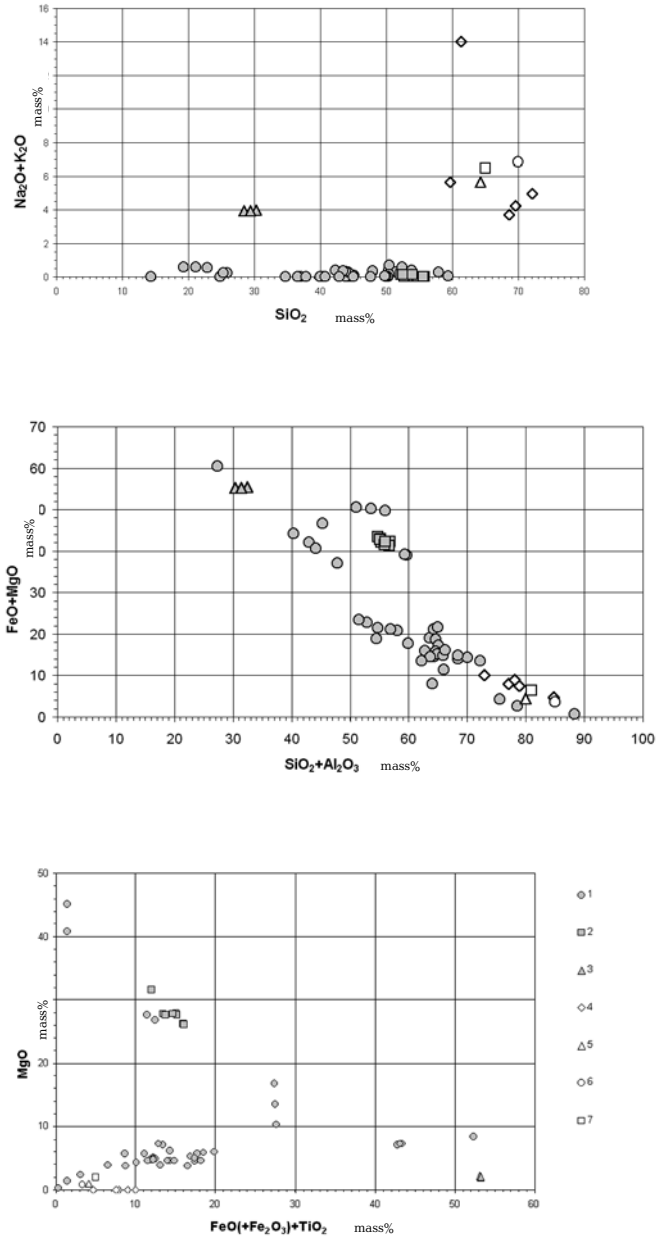

Fig. 2. Variational diagram of alumosilicate glass compositions: 1 — Nezhdaninskoye deposit, 2 — Democrat, 3 — Kellyam, 4 — Kokpatas, 5 — hosting siltstones, Nezhdaninskoye, 6 — hosting sandstones, Nezhdaninskoye, 7 — granodiorite, average after R.A. Daly.

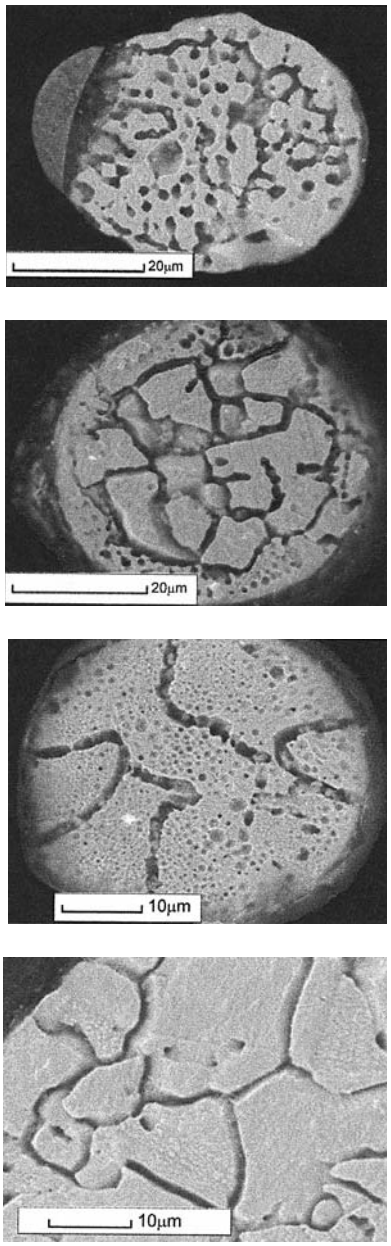

Fig. 3. Contraction cracks seen in a cross section of a native gold microspherula. SEM.

ence of natural fluxes and subsequent liquation of ore micromelts) and 650 — 400°C (fusion of galena-antimonite mixture with formation of boulangerite and galena through eutectoid disintegration of falkmanite protocompound) and to 300 — 250° C (fusion, stratification and eutectoid disintegration with formation of Au-Pb-Sb phases).

The fugitivity of sulfur and oxygen in gas phase equilibrated with sulfides of Pb and Sb was calculated by tabulated values of free Gibbs energy in reactions of sulfidization and

Table 1. **Chemical composition (wt. %) of microspherula minerals**

№	Mineral	Sample	Number of analyses	Au	Ag	Pb	Sb	Fe	As	S	Total	Formula
1	Arsenopyrite	92	3	–	–	–	–	34.39	46.23	19.52	100.14	$Fe_{1.00}As_{1.00}S_{1.00}$
2	–''–	82	5	–	–	–	–	34.32	45.99	19.79	100.10	$Fe_{1.00}As_{1.00}S_{1.00}$
3	Pyrite	–"–	5	0.2	–	–	0.2	46.70	–	48.8	95.9	$Fe_{1.06}S_{1.93}$
4	Pyrrhotite	–"–	2	–	–	–	0.2	63.60	0.7	34.8	99.3	$Fe_{1.02}S_{0.97}As_{0.01}$
5	Antimonite	–"–	3	0.2	–	–	69.6	0.30	0.5	27.9	98.5	$Sb_{1.95}S_{3.00}$
6	Galena	–"–	6	0.7	1.0	83.3	0.2	–	0.5	13.4	99.1	$Pb_{0.96}Ag_{0.02}Au_{0.01}$ $S_{0.99}As_{0.02}$
7	Galena	105	1	–	–	86.58	–	–	–	14.03	100.61	$Pb_{0.98}S_{1.02}$
8	–"–	90	1	–	–	87.24	–	–	–	14.18	101.42	$Pb_{0.98}S_{1.02}$
9	–"–	96	1	–	–	86.32	–	–	–	14.05	100.37	$Pb_{0.98}S_{1.02}$
10	–"–	82	4	–	–	86.52	–	–	–	13.59	100.11	$Pb_{0.99}S_{1.01}$
11	–"–	109	4	–	–	86.70	–	–	–	13.63	100.33	$Pb_{0.99}S_{1.01}$
12	–"–	62	2	–	–	86.49	–	–	–	13.71	100.20	$Pb_{0.99}S_{1.01}$
13	Boulangerite	82	4	–	–	55.46	25.55	–	–	18.83	99.84	$Pb_{5.03}Sb_{3.94}S_{11.03}$
14	–"–	109	4	–	–	55.54	25.38	–	–	19.12	100.04	$Pb_{5.00}Sb_{3.89}S_{11.11}$
15	–"–	–"–	4	0.3	–	56.9	24.1	–	1.4	17.6	100.30	$(Pb_{5.27}Au_{0.03})_{5.30}$ $Sb_{3.80}As_{0.36}S_{10.54}$
16	Gold	92	3	77.70	21.95	–	–	–	–	–	99.65	$Au_{1.98}Ag_{1.02}$
17	–"–	105	2	78.82	20.62	–	–	–	–	–	99.44	$Au_{2.03}Ag_{0.97}$
18	–"–	96	1	84.97	14.46	–	–	–	–	–	99.43	$Au_{3.05}Ag_{0.95}$
19	–"–	–"–	2	82.92	16.21	–	–	–	–	–	99.13	$Au_{2.96}Ag_{1.03}$
20	–"–	–"–	2	92.72	6.96	–	–	–	–	–	99.68	$Au_{3.52}Ag_{0.48}$
21	–"–	90	4	75.69	23.47	–	–	–	–	–	99.16	$Au_{1.92}Ag_{1.08}$
22	–"–	–"–	1	68.60	30.97	–	–	–	–	–	99.57	$Au_{1.10}Ag_{0.90}$
23	Au–Pb–Sb	92	1	70.98	–	2.90	25.08	–	–	–	98.96	$Au_{0.72}Sb_{0.23}Pb_{0.03}$
24	–"–	62	3	42.46	–	12.06	45.65	–	–	–	100.17	$Au_{0.33}Sb_{0.58}Pb_{0.09}$
25	–"–	–"–	3	41.89	–	44.30	13.58	–	–	–	99.77	$Au_{0.39}Sb_{0.21}Pb_{0.40}$
26	–"–	–"–	5	42.3	0.6	45.3	11.3	–	1.1	–	100.6	$Au_{0.39}Ag_{0.01}Pb_{0.40}$ $Sb_{0.17}As_{0.03}$
27	–"–	–"–	3	74.9	4.0	1.8	19.6	–	1.3	–	101.6	$Au_{0.63}Ag_{0.06}Pb_{0.01}$ $Sb_{0.27}As_{0.03}$
28	–"–	–"–	3	62.8	1.1	0.9	31.1	–	3.3	–	99.2	$Au_{0.50}Ag_{0.02}Pb_{0.01}$ $Sb_{0.40}As_{0.07}$
29	Arsenic	–"–	4	2.1	–	0.4	1.3	–	96.1	–	99.9	$As_{0.98}Sb_{0.01}Au_{0.01}$
30	Au–Sb–As	–"–	3	59.2	–	0.9	25.1	–	14.9	–	100.1	$Au_{0.42}Pb_{0.01}Sb_{0.29}As_{0.28}$
31	Ag–Pb–S	105	1	–	24.24	60.72	–	–	–	15.91	100.87	$Pb_{0.58}Ag_{0.44}S_{0.98}$
32	–"–	–"–	1	–	19.45	65.16	–	–	–	15.30	99.90	$Pb_{0.63}Ag_{0.37}S_{0.98}$
33	–"–	–"–	1	–	22.10	62.86	–	–	–	15.43	100.39	$Pb_{0.61}Ag_{0.41}S_{0.97}$
34	Sb–As	125	3	–	–	–	51.63	–	49.00	–	100.63	$As_{3.03}Sb_{1.97}$
35	Pb–Sb–Fe–0 (PbO)	90 (Sb_2O_5)	1 (FeO)	– $O_{4.02}$	–	72.54	20.38	6.14	–	–	99.07	$Pb_{1.83}Sb_{1.71}Fe_{0.48}$

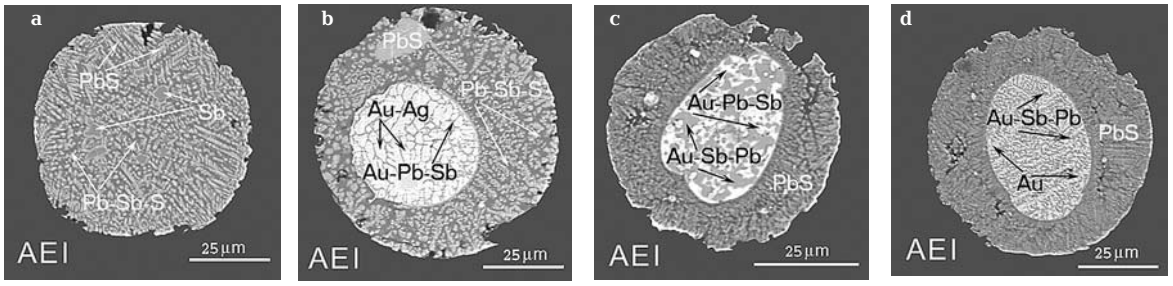

Fig. 4. *Structure of ore microspherulas in section: galena dendrites in boulangerite matrix with irregular segregations of native antimony rimed by galena (a); zonal microspherulas with «gold» core: eutectoid aggregates of gold and Au-Pb-Sb phases with galena-boulangerite rim with a relic of unmelted galena (b); eutectoid aggregates of Au-Pb-Sb phase differing in Pb contents in galenite matrix with an admixture of boulangerite (c); sliced structures of Au-Pb-Sb phase and Au in «gold» core with galenite-boulangerite rim (d). The image in absorbed current (AEI). The scale ruler is 25 μm. Kellyam deposit.*

oxidation (Novgorodova *et al.*, 2003$_2$). It was shown that the gas phase (molar shares of H_2>H_2O>H_2S) is saturated with hydrogen.

The initial stage of microspherula formation is the process of fusion of solid particles presenting as a suspension in the hydrothermal solution and got in cavitation field. Solid particles may form initial centers of cavitation bubbles. A necessary condition of transition of solid particles into the melt drops is the increase of their temperature up to values exceeding the fusion point. Such increase may be realized at collapse of a vapor-gas bubble. However, microsecond duration of the process requires discussion of its dynamics, amount of emitted energy and speed of solid particle heating.

Necessary calculations were made for quartz and gold, the most refractory minerals present in microspherulas, without taking into account natural additives decreasing fusion points. In other words, the task was to estimate the impact of maximum possible temperatures quickly arising at cavitation phenomena. For calculations, it was accepted that initial pressure P_1 is 1.5 kbar, T is 250° C, gas bubbles during their maximal expansion have centimetric sizes, the size of native gold micrograins is 50 μm, that of quartz 10 μm. For simplification, it is also accepted that the liquid phase is water.

To evaluate the dynamics of gas-vapor bubble collapse in water we used the Rayleigh equation (Naugol'nykh and Ostrovsky, 1990):

$$R\frac{d^2R}{dt^2}+\frac{3}{2}\left(\frac{dR}{dt}\right)^2=\frac{1}{\rho_l}\left(P(t)-P_1\right), \qquad (1)$$

where R — bubble radius, P(t) and P_1 — pressure inside the bubble and initial pressure respectively, ρ_1 — density of incompressible liquid environment of the bubble. Pressure P(t) was defined under formulas of adiabatic compression of non-ideal gas described by the Van der Vaals equation with a variable thermal capacity in calculation to one particle $C_v = 5/2$ for density of vapor $\rho_v < \rho_c$ less than critical density ρ_c and $C_v = 3$ for density $\rho_v > \rho_c$.

The calculation under the formula (1) at P_1 = 1.5 kbar, ρ_1 = 1 g/cm^3 and initial conditions P_0 = 40.5 bar and R_0 = 1 cm, where P_0 — pressure of saturated vapor at 250° C, R_0 — radius of expanded bubble, shows that time t_m of existence of high temperature $T > T_f$ in a bubble does not exceed 1.5 ms. The maximum temperature can rich T_{max} = 7030° C and minimum radius of a bubble R_{min} = 0.15 cm. Values t_m and R_{min} appear approximately proportional to the initial radius of a bubble, at the same time T_{max} almost does not depend on R_0.

Elementary evaluation of $l=\sqrt{\chi t}$ n case of quartz micrograin (thermal diffusivity χ = 0.02 cm^2/s) shows that in time t ~1 ms the thickness of fused layer is relatively small l ~1.7 μm, as comparison with the micrograin radius r_s = 10 μm. At the same time, the appreciable excess of T_{max} over fusion point may provide energy input sufficient for deeper fusion of micrograins.

Solving the equation of heat conductivity for a spherical quartz microparticle with given thermal diffusivity χ, thermal capacity C_s = 70 Joule/(Mole •°C), fusion point T_f = 1610°C and initial temperature $T_{(r,o)}$ = 250° C, which surface temperature T_s = T(t) is determined from the decision of equation (1), it is possible to find out the complete energy input and distribution of temperature inside the micrograin at the given moment of time (Carslow, Eguer, 1964). Fig. 5 shows the complete energy input

$$\Delta Q = 4\pi c_s \int_0^{r_s} (T(r)-T_0)r^2 dr$$

and thickness of fused layer Δr in dependence on radius of extended cavitation bubble to the moment of time, when the bubble temperature T(t), after having past the maximum T_{max} = 7030° C, decreases to the value $T(t) = T_f$.

In Fig. 5 it is visible that the micrograin receives the energy necessary for its complete fusion ΔQ = 161 erg at R_0 = 1.4 cm, but actual temperature distribution is essentially irregular and the thickness of a fused layer at this moment only makes Δr = 3.7 μm. At the subsequent moments of time the fusion depth may increase to 4.5 μm. Full fusion may be realized at $R_0 > 2$ cm.

Thus, the quartz micrograin 10 μm in size may be «dry» melted due to thermal energy arising at sharp adiabatic reduction of gas bubble with radius from 2 cm to 0.6 cm. So high temperatures (quartz T_f = 1610° C) initiating the fusion of quartz micrograin surface may only be realized at centimetric sizes of extended gas bubble, that is apparently possible only at big volume of adiabatic cavity.

Similar calculations were also made for a 50 μm native gold micrograin (T_f = 1063° C, Cs = 25.23 Joule/(Mole • °C), χ = 1 cm^2/s), which results are shown in Fig 6. In this case the necessary for complete fusion energy input ΔQ = 1.06·104 erg is reached at R_0 = 0.2 cm. At this, R_{min} = 0.06 cm and fusion depth Δr = 14 μm. The complete fusion of native gold micrograin within the framework of the given model requires $R_0 > 0.5$ cm.

Equation (1) shows that temperature of solid particle and energy input of a compressed bub-

Table 2. **Invariant points of a natural system with Au, Pb, Sb, S, As, Fe**
(after Robinson, 1948; Craig *et al.*, 1973; Gmelin Handbook...,1996)

Low-temperature association	High-temperature association	T°C
Quartz	Melt	1610
Galena	Melt	1115
Gold	Melt	1063.4
Galena-lead	Melt (stratified)	1041
Bronzite	Melt (1 kbar)	850
Antimony-melt (56% S)	Monotectic melt (~5,5% S)	800
Pyrite (+ sulfur)	Melt	743
Arsenopyrite	Pyrrhotite + loellingite + melt	702
Falkmanite (phase I after Craig et al.)	Galena + melt, Rich Sb_2S_3	642
Boulangerite	Falkmanite (phase I after Craig *et al.* 1973)	638
Gold − arsenic	Eutectic melt	636
Galena + antimony	Melt	622
Antimonite + antimony	Melt (stratified)	615
Boulangerite + galena	Falkmanite (phase I after Craig *et al.* 1973)	605
Ag_2S + galena	Melt	605
Arsenic (25.5 %) + Antimony	Eutectic melt	602
Antimonite	Melt	556
Pyrite + arsenopyrite	Pyrrhotite + melt (AsS)	491
Aurostibite	Melt (congruent fusion)	460
Gold + silicon (6%)	Eutectic melt	370
Gold-aurostibite	Eutectic melt	360
Phase $Au_{0,36}Pb_{0,25}Sb_{0,39}$	Eutectic melt	250

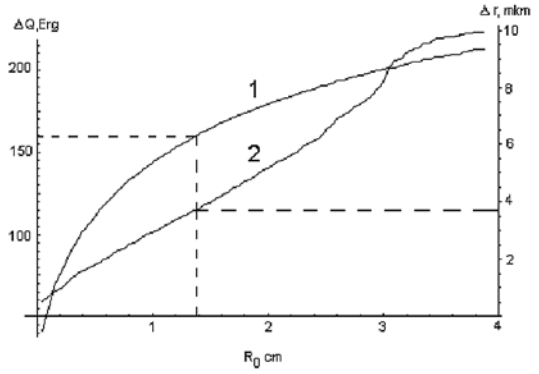

Fig. 5. *Energy input ΔQ, erg (Curve 1) and melted layer thickness Δr, micrometers (Curve 2) in quartz micrograins versus radius of vapor-gas bubble at its expansion*

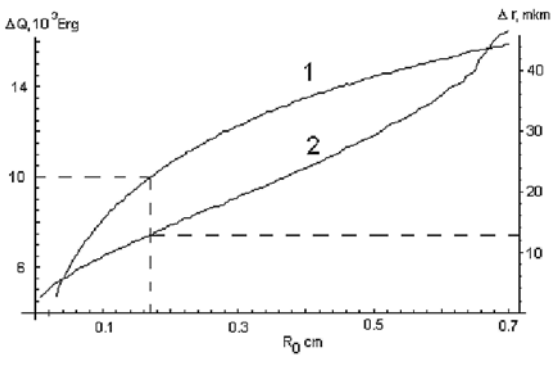

Fig. 6. *Energy input ΔQ, erg (Curve 1) and melted layer thickness Δr, micrometers (Curve 2) in gold micrograins versus initial radius of vapor-gas bubble*

ble depend on its size at the moment of its greatest expansion. It is natural that more fusible matter of the majority of mineral microspherulas (Tables 1, 2) require 1—2 orders smaller bubbles.

It is necessary to remember that the used model is rather simplified and requires a number of specifications, in particular, more consistent consideration of dynamics of boundary processes liquid/vapor, real equation of state and process of heat transfer from the environment to a micrograin.

Nevertheless, the probability of sharp temperature fluctuations accompanied with generation of thermal energy sufficient for melting solid particles in a flow of boiling up hydrothermal solution is proved by the above calculations of cavitation models.

The work was executed at the financial support of the RFRI, grant 00-05-64709.

References

Bortnikov N.S., Gamjanin G.N., and Alpatov V.A. Mineralogo-geokhimicheskie osobennosti i usloviya obrazovaniya Nezhdaninskogo mestorozhdeniya zolota (Sakha-Yakutiya, Rossiya) (Mineralogical-geochemical features and conditions of formation of the Nezhdaninskoye gold deposit (Sakha-Yakutia, Russia) // Geol. Rudn. Mestor., **1998**. V. 40. #2. P 137—156. (Rus.)

Carslow G. and Eguer D. Teploprovodnost tverdykh tel (Heat conductivity of solid bodies) // M., Science, **1964**.(Rus.)

Craig J.R., Chang Z.Z.Y., Zeees W.R. Investigations in the Pb-Sb-S system // Canad. Mineral. **1973**. Vol. 12. Part 3. P. 199—206.

Dilabio R.H.W., Newsame J.W., Mc Jvor D.F., Jowenstein P.J. The shperoid form of gold: manmade or secondary // Ecom. Geol. **1988**. V 83. P. 153-162.

Frost B.R., Mavrogenes J.A., Tomkins A.G. Partial melting of sulfide ore deposits during medium — and high-grade metamorphism // Can. Mines. **2002**. V 40. P. 1. P. 1—18.

Gamyanin G.N., Zhdanov Yu.Ya., and Syromyatnikova A.S. Sostav i strukturnye osobennosti sferoidov iz zolotorudnykh mestorozhdenii Vostochnoi Yakutii (Composition and structural features of spheroids from gold-ore deposits of East Yakutia) // ZVMO. **1999**. Part. 128. #5. P 71—75. (Rus.)

Gmelin Handbook of inorganic and organom etallic chemistry // An. Suppl. **1996**. Vol. 134. P.128—134.

Naugol'nyh K.A. and Ostrovsky L.A. Nelineinye volnovye protsessy v akustike (Nonlinear wave processes in acoustics) // M.: Science, **1990**. (Rus.)

Novgorodova M.I., Gamyanin G.N., Zhdanov Yu.Ya., Agakhanov A.A., and Dikaya T.V. Mikrosferuly alyumosilikatnykh stekol v zolotykh rudakh (Microspherulas of alumosilicate glasses in gold ores) // Geochemistry. **2003$_1$**. #1. (Rus.)

Novgorodova M.I., Gamyanin G.N., Zhdanov Yu.Ya., Agakhanov A.A., and Dikaya T.V. Mikrosferuly samorodnogo zolota, sulfidov i sulfosolei v zolotykh rudakh (Microspherulas of native gold, sulfides and sulfosalts in gold ores) // Geochemistry. **20032** (in press). (Rus.)

Robinson S.C. Synthesis of Lead Sulphantimonites // Econ. Geol. **1948**. Vol. 43. No 4. P. 293—312.

Vernadsky V.I. Izbrannye sochineniya. (Selected works of V.I.Vernadsky) (v. 1, 2). // M.: Publishing House of the RAS of the USSR, **1955**. 615 p. (Rus.)